



LUND UNIVERSITY

Tackling the Uncertainties of Event Generators

Gellersen, Leif

2021

Document Version:

Publisher's PDF, also known as Version of record

[Link to publication](#)

Citation for published version (APA):

Gellersen, L. (2021). *Tackling the Uncertainties of Event Generators*. Lund University (Media-Tryck).

Total number of authors:

1

General rights

Unless other specific re-use rights are stated the following general rights apply:

Copyright and moral rights for the publications made accessible in the public portal are retained by the authors and/or other copyright owners and it is a condition of accessing publications that users recognise and abide by the legal requirements associated with these rights.

- Users may download and print one copy of any publication from the public portal for the purpose of private study or research.
- You may not further distribute the material or use it for any profit-making activity or commercial gain
- You may freely distribute the URL identifying the publication in the public portal

Read more about Creative commons licenses: <https://creativecommons.org/licenses/>

Take down policy

If you believe that this document breaches copyright please contact us providing details, and we will remove access to the work immediately and investigate your claim.

LUND UNIVERSITY

PO Box 117
221 00 Lund
+46 46-222 00 00

Tackling the Uncertainties of Event Generators

LEIF GELLERSEN

FACULTY OF SCIENCE | LUND UNIVERSITY





Faculty of Science
Department of Astronomy
and Theoretical Physics

ISBN 978-91-8039-054-5



Tackling the Uncertainties of Event Generators

Tackling the Uncertainties of Event Generators

by Leif Gellersen



LUND
UNIVERSITY

Thesis for the degree of Doctor of Philosophy

Thesis advisors: Malin Sjödahl, Stefan Prestel

Faculty opponent: Jennifer Smillie

To be presented, with the permission of the Faculty of Science of Lund University,
for public criticism in Lundmarksalen at the Department of Astronomy and Theoretical Physics
on Thursday the 25th of November 2021 at 10:00.

Organization LUND UNIVERSITY Department of Astronomy and Theoretical Physics Sölvegatan 14A SE-223 62 Lund Sweden		Document name DOCTORAL DISSERTATION	
		Date of disputation 2021-11-25	
Author(s) Leif Gellersen		Sponsoring organization	
Title and subtitle Tackling the Uncertainties of Event Generators			
Abstract <p>This thesis is composed of four papers, which concern Monte Carlo event generators for high energy particle physics. Precise predictions of the outcome of particle collisions are important for the exploration of the Standard Model of particle physics at collider experiments like the LHC at CERN. The papers address the uncertainties of these predictions in different contexts.</p> <p>Paper I presents an algorithm for tuning Monte Carlo event generators with high dimensional parameter spaces by splitting the parameter space algorithmically. The algorithm is tested in ideal conditions and real-life examples of tuning HERWIG and PYTHIA for LEP.</p> <p>Paper II concerns the perturbative uncertainty of unitarized next-to-leading order multi-jet merging prescriptions by discussing scale variations and scheme variations. The uncertainties are addressed for collisions at LEP and LHC.</p> <p>Paper III deals with QCD/QED interference effects in parton showers. For this purpose, we implement a shower including QED and QCD emissions and tree-level matrix element corrections for fixed color configurations.</p> <p>Paper IV proposes a method for the consistent removal of overlapping singularities in QCD parton showers at next-to-leading order in the strong coupling.</p>			
Key words QCD, Phenomenology, Parton Showers, Matrix Element Merging, Tuning			
Classification system and/or index terms (if any)			
Supplementary bibliographical information		Language English	
ISSN and key title		ISBN 978-91-8039-054-5 (print) 978-91-8039-053-8 (pdf)	
Recipient's notes		Number of pages 166	Price
		Security classification	

I, the undersigned, being the copyright owner of the abstract of the above-mentioned dissertation, hereby grant to all reference sources the permission to publish and disseminate the abstract of the above-mentioned dissertation.

Signature 

Date 2021-10-15

Tackling the Uncertainties of Event Generators

by Leif Gellersen



LUND
UNIVERSITY

A doctoral thesis at a university in Sweden takes either the form of a single, cohesive research study (monograph) or a summary of research papers (compilation thesis), which the doctoral student has written alone or together with one or several other author(s).

In the latter case the thesis consists of two parts. An introductory text puts the research work into context and summarizes the main points of the papers. Then, the research publications themselves are reproduced, together with a description of the individual contributions of the authors. The research papers may either have been already published or are manuscripts at various stages (in press, submitted, or in draft).

Cover illustration front: Forest on Rügen, autumn 2015.

Funding information: This work has received funding from the European Union's Horizon 2020 research and innovation programme as part of the Marie Skłodowska-Curie Innovative Training Network MCnetITN₃ (Grant agreement no. 722104).

© Leif Gellersen 2021

Faculty of Science, Department of Astronomy and Theoretical Physics

ISBN: 978-91-8039-054-5 (print)

ISBN: 978-91-8039-053-8 (pdf)

Printed in Sweden by Media-Tryck, Lund University, Lund 2021



Media-Tryck is a Nordic Swan Ecolabel certified provider of printed material. Read more about our environmental work at www.mediatryck.lu.se

MADE IN SWEDEN 

To my family

Contents

List of publications	iii
Popular Summary	iv
Introduction	I
1 Particle Physics and the Standard Model	I
2 Matrix Elements and Cross Sections	10
3 Parton Showers	14
4 Matching and Merging	22
5 Monte Carlo Event Generator Tuning	29
6 Outlook	30
7 Overview of Publications	31
8 Acknowledgements	34
Publications	
I High dimensional parameter tuning for event generators	41
1 Introduction and Motivation	42
2 Current State	43
3 The Algorithm	45
4 Testing and Findings	51
5 Results	54
6 Conclusion and Outlook	57
A Range Dependence	58
B Tune Results	60
II Scale and scheme variations in unitarized NLO merging	71
1 Introduction	72
2 Unitarized NLO-merged calculations	73
3 Theory and Implementation	75
4 Application and Results	85
5 Summary and Outlook	93
6 Acknowledgments	95
A Implementation Details	95

III	Coloring mixed QCD/QED evolution	105
1	Introduction	106
2	Implementation	107
3	Results	117
4	Conclusions and Outlook	123
5	Acknowledgments	124
A	Implementation details	124
IV	Disentangling soft and collinear effects in QCD parton showers	131
1	Introduction	132
2	Strategy for constructing an NLO parton shower	133
3	Parton evolution in the triple collinear and double soft limits	135
4	Overlap removal and genuine collinear anomalous dimension	137
5	Computation in four dimensions	140
6	Relation to the effective soft-gluon coupling	141
7	Numerical results	144
8	Conclusions	145
9	Acknowledgments	146
A	Implementation of symmetry factors	146

List of publications

This thesis is based on the following publications, referred to by their Roman numerals:

- I **High dimensional parameter tuning for event generators**
Johannes Bellm, Leif Gellersen
Eur.Phys.J.C 80 (2020) 1, 54. E-print: arXiv:1908.10811 [hep-ph]

- II **Scale and scheme variations in unitarized NLO merging**
Leif Gellersen, Stefan Prestel
Phys.Rev.D 101 (2020) 11, 114007. E-print: arXiv:2001.10746 [hep-ph]

- III **Coloring mixed QCD/QED evolution**
Leif Gellersen, Stefan Prestel, Michael Spannowsky
To be submitted to SciPost Phys. E-print: arXiv:2109.09706 [hep-ph]

- IV **Disentangling soft and collinear effects in QCD parton evolution**
Leif Gellersen, Stefan Höche, Stefan Prestel
To be submitted to Phys.Rev.D. E-print: arXiv:2110.05964 [hep-ph]

Popular Summary

The field of elementary particle physics is driven by the desire to understand the most fundamental building blocks of nature and how they interact. One very successful way to experimentally access the properties of elementary particles is to accelerate them to very high energies and let them collide, as it is done at the Large Hadron Collider at CERN near Geneva. According to Einstein's famous equation $E = mc^2$, the kinetic energy of the colliding particles can be converted to mass and form new particles. The properties of the particles produced in collisions can be measured and studied. In this way, we can learn more about the properties of known particles and their interactions, or even find new ones.

The accelerated particles move with velocities close to the speed of light. To describe these particles appropriately, we need to use Einstein's theory of Special Relativity. The high collision energies also imply that the scattering process happens at very short time scales, corresponding to small distances. This aspect is captured by Quantum Mechanics, giving rise to a probabilistic outcome of experiments even if the initial conditions are identical. These theories are combined in Quantum Field Theory, where particles are described in terms of fields.

The Standard Model of particle physics is a very successful quantum field theory that describes all elementary particles that have been discovered so far. It includes three of the four fundamental forces, the electromagnetic force, the weak force and the strong force. Electromagnetism describes the interactions between particles with electric charge, and is responsible for the visible light. The weak force governs certain types of radioactive decays, while the strong force is responsible for the stability of atomic nuclei. The gravitational force is not described by the Standard Model, but it is typically much weaker than the other forces at particle-physics experiments, such that the Standard Model still gives very accurate predictions.

Once the free parameters of the Standard Model are measured experimentally, it allows to predict the outcome of many experiments. However, the theory is very complex, and different assumptions, approximations and additional modeling need to be combined to describe the outcome of collider experiments on the level of individual outgoing particles. Monte Carlo Event Generators allow for the simulation of collision events based on random numbers, reflecting the probabilistic nature of such processes. Combining a large number of these generated events gives rise to probabilistic distributions that can be compared to experimental data. Based on this comparison, it is possible to determine parameters of the underlying theory and improve the modeling of events. Furthermore, the predictions can provide guidance on how to design experimental analyses, e.g., by estimating backgrounds to signals of interest. The precise simulation of the existing theory might thus allow for the identification of experimental signals that are not compatible with the known theories,

pointing to new phenomena that the Standard Model might not be able to describe.

The publications in this thesis concern some of the uncertainties and assumptions associated with Monte Carlo event generators. The first publication proposes a method for the optimization of parameters to better describe data, especially in the case that many parameters need to be optimized. The second publication addresses uncertainties in the combined description of the hard process at the core of a collision, and the radiation of further particles from the incoming and outgoing particles. The third publication concerns the interference between electromagnetic and strong radiation effects in combination with an improved modeling of the strong radiation. The fourth publication is about the consistent combination of precision effects in different limits of the emission of pairs of particles in a radiative cascade.

Introduction

This thesis collects my work during my studies in Lund in the field of high energy particle physics. The four included publications address different aspects of Monte Carlo Event Generators (MCEGs), which are used to simulate particle collision events at collider experiments like the Large Hadron Collider at CERN. Precise predictions of the expected outcome of collisions are crucial to explore the Standard Model of particle physics and to identify collision events that might signal new physics. As the field is rather established, some background in particle physics is required to understand the content of the publications, and a thorough introduction that would make them accessible to all readers is beyond the scope of this thesis. The introduction therefore starts at a general level, and then becomes more technical to provide some context for the research papers. Thorough introductions to Quantum Field Theory and the Standard Model can be found in [1, 2], a detailed description of Quantum Chromodynamics and hadron collider physics is available in [3], and a review on general-purpose event generators for LHC physics is given in [4].

The first section of the introduction gives a brief introduction into particle physics, the Standard Model and its application to collider physics by means of simulating particle collision events using MCEGs. Starting from section two, the introduction becomes more technical, introducing cross sections and matrix elements as the central concepts when calculating the probability of observing certain collision events. Sections three and four of the introduction introduce parton showers and the matching and merging of parton showers with matrix elements, providing some background for Papers II, III and IV. Section five briefly touches upon the tuning of Event Generators, which is the topic of Paper I. The introduction concludes with an outlook and an overview of the publications included in this thesis.

I Particle Physics and the Standard Model

The field of theoretical physics is driven by the motivation to describe the world based on fundamental mathematical principles. This applies to a vast range of resolution scales. In

one extreme, the theory of general relativity describes gravitation on galactic scales, treating space and time as a dynamic ensemble curved by energy. It allows to describe the motion of planets and whole galaxies, and gravitational waves emerging from rapidly accelerated massive objects. In the other extreme, the fundamental building blocks of nature are described by the theory of quantum fields, treating elementary particles as excitations of fields that obey the rules of special relativity and quantum mechanics.

The field of classical mechanics, which is the traditional theory applicable at human and planetary scales, describes the dynamics of objects based on forces. By measuring the forces acting on objects, one can describe accelerations of objects and thus how they move and interact. In order to determine the force that two electrically charged objects exert on each other, we can for example place these objects at different distances to each other and measure the force between the two depending on how far they are apart.

Compared to everyday scales, elementary particles are very light and small, which means that the rules of classical mechanics are not sufficient to describe their dynamics. Accelerating particles to high energies leads to very high velocities. This is the regime of special relativity, which combines space and time into a united framework. Energy and momentum are conserved, but the concept of mass becomes broader. Massless particles like the photon can travel at the speed of light. In decays of massive particles, mass of bound states can be converted to kinetic energy, making mass just one incarnation of different forms of energy, and giving rise to Einstein's famous equation $E = mc^2$ [5].

Looking at very small systems also necessitates taking into account the results of quantum mechanics. Small systems can be characterized by states, and the behavior of systems determined by transition probabilities between different such states. The probability of going from one state to another can only be described probabilistically. Looking for example at the transition of a bound state to a more stable state in a radioactive decay, we can only determine the probability of this transition to occur in a given amount of time, and by observing such a transition very often, we recover a probability distribution. However, it is not possible to determine the exact lifetime of a specific nucleus, only the probability distribution governing the decay process.

The fundamental question that we try to answer in particle physics is: *What are we made of?* Everything we experience in our daily lives can be broken down into the dynamics of smaller systems. We are built according to information encoded in our genome, which consists of amino acids. Those are complex molecules, formed from atoms. The atoms in turn are composed of electrons, protons and neutrons. Protons and neutrons can further be broken down into quarks, ultimately giving a set of elementary particles. While everyday phenomena are thus fundamentally governed by the rules of elementary particles, the rather complex calculations necessary to compute the behavior of systems with many particles means that they can not be applied directly, motivating the use of effective theories at

different scales. By understanding how elementary particles interact with each other, we hope to understand on the most fundamental level why the world behaves like it does.

On the scales of particle physics, the objects of interest are typically way too small to measure the forces directly. Instead, if we want to understand how elementary particles interact with each other, we have to find other ways of experimentally accessing their properties. On the scale of atoms, the dynamics are governed by how electrons are bound to the nucleus due to the electromagnetic force. On an even smaller scale, we can study the composition of hadrons, which are bound by the strong force to form nuclei. Another approach is to look out for the decay of bound states. The radioactive β -decay of neutrons into protons, electrons and neutrinos, allows us to access properties of the weak force. A powerful approach to access the detailed dynamics of the electromagnetic, weak and strong forces is to perform collisions of particles. By studying the outcome of different types of collision experiments, we can learn about the composition of composite particles, and about the properties of elementary particles alike.

In elementary particle physics, Quantum Field Theory (QFT) allows us to describe the dynamics of elementary particles in terms of excited fields. Excitations of these fields correspond to particles, and their dynamics are compatible with the predictions of quantum mechanics and special relativity. The Standard Model of particle physics is based on the language of QFT, and is in fact a collection of related theories, including Quantum Electrodynamics (QED), the Glashow-Weinberg-Salam theory of electroweak processes and the theory of Quantum Chromodynamics (QCD). It is very successful in describing a large variety of phenomena to an astonishing precision.

However, the Standard Model can hardly be seen as the final word in particle physics, since it is an effective theory with many parameters, the values of which are not determined by the theory itself.

In order to improve our understanding of particle physics, there are multiple ways to go about it. We can extend the Standard Model to include new physics, which are not (yet) described by the Standard Model, called Beyond the Standard Model (BSM) physics. Many efforts are also put into finding an even more fundamental theory, of which the Standard Model can be derived as a low-energy approximation. In order to determine what kinds of improvements are required, it is important to study the phenomenology of the Standard Model in detail and to perform precision calculations within the Standard Model. Only such predictions allow to compare experimental observations to the Standard Model, and identify effects that might not be described appropriately.

The projects included in this thesis all lie within the last mentioned category, facilitating precise predictions based on the Standard Model, which can then be compared to experimental results. This comparison enables us to determine deviations between the theoretical predictions of the Standard Model and the observed behavior of high-energy particle phys-

ics experiments.

1.1 The Standard Model

The Standard Model of particle physics collects the fundamental particles and describes their interactions. The fundamental particles described by the Standard Model can be summarized as follows:

Fermions The group of fermions consists of quarks and leptons, and together, these form the constituents of the matter we observe. While three generations of fermions exist, only the first and lightest generation occurs abundantly in everyday life. The up and down quarks form protons and neutrons, which together form the cores of atoms. The electron and its neutrino form the lightest generation of leptons. While the electron, together with the cores, forms electrically neutral atoms, there is also its neutrino, which is less visible due to the lack of electric charge.

Bosons The symmetry properties of the Standard Model give rise to the existence of gauge bosons, which describe the forces between fermions. There are three gauge forces in the Standard Model. Electromagnetism is mediated by the photon, and describes the forces acting on electrically charged fermions. The weak force, mediated by W^\pm and Z bosons, is crucial for describing the radioactive β -decay. Finally, there is the strong force, mediated by gluons. Just like the photons, gluons are massless, but unlike their electromagnetic counterpart, they can interact with each other. Finally, there is the Higgs boson. Its interaction with the fermions gives rise to the masses of elementary particles.

The particle content and its interactions are shown in Fig. 1.

The formulation of the Standard Model is based on the identification of symmetries that give rise to conserved quantities, the charges. Specifying all symmetries of the theory allows to write down the Lagrangian density, including all terms that obey the specified symmetries. From this function, the equations of motion can be derived, ultimately describing how the theory behaves. Taking the example of the complex electron field Ψ , which comes with an absolute value ψ and a phase ϕ : $\Psi = \psi e^{i\phi}$. The $U(1)$ symmetry transformation of the field is given by $\Psi \mapsto e^{i\phi(x)}\Psi$, where the dependence on the space-time point x characterizes a *local* symmetry transformation. Assuming that this symmetry transformation should leave the predictions of the theory invariant requires the introduction of additional terms in the Lagrangian density, compensating for the effect of the transformation. These terms, together with a kinetic term to describe the free behavior of the introduced field $\phi(x)$, then gives the gauge theory describing the photon, QED.

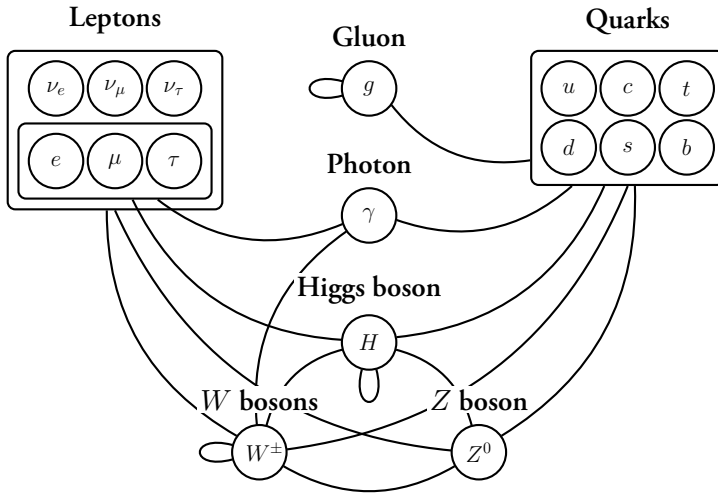


Figure 1: Particle content of the Standard Model. The lines indicate interactions. All electrically charged particles interact with the photon. All color charged particles interact with the gluon, including itself. Both Leptons and Quarks interact with W and Z bosons. The Higgs boson couples to all massive particles.

A similar reasoning can be applied to other local gauge symmetries, namely $SU(2)_L \otimes U(1)_Y$, giving rise to the model of electroweak interactions, where all fermions except the neutrino come in left- and right-handed versions, with only the left-handed transforming under the $SU(2)_L$ symmetry transformation. This symmetry actually includes QED, which only becomes apparent when the original symmetries are hidden by the Higgs mechanism. The $SU(3)_C$ symmetry group gives rise to QCD, where the C stands for color, the charge of the strong force. Only the quarks are affected by the $SU(3)_C$ group, while all fermions take part in the electro-weak interaction.

Once the Standard Model Lagrangian density is constructed, it becomes apparent that it depends on about 25 parameters, describing the masses and interactions of the fields. These can be determined from experiments, allowing us to use the theory to make various predictions. In practice, these predictions are usually limited to small systems with a limited number of involved particles.

Nevertheless, the Standard Model has been very successful. It allowed for the prediction of different quarks and bosons before their first observations. With the discovery of the Higgs boson in 2012 [6, 7], all particles predicted by the Standard Model have been observed experimentally. Beyond the existence of particles, the model allows for the precise prediction of various observables at collider experiments and beyond.

1.2 Limitations and Open Questions

While the Standard Model is extremely successful in describing a large range of experimental results very precisely, there are also limitations and open questions to which it cannot provide an answer. One question that remains unsolved is why the Standard Model takes the form it has. While experiments dictate the symmetries and values of parameters needed to describe elementary particles, the Standard Model does not provide an answer to the question why exactly these symmetries are realized in nature, and why exactly three generations of fermions exist. Also, the hierarchy between the different generations' fermion masses is not explained within the Standard Model. It is therefore desirable to embed the Standard Model into an overarching framework that gives answers to these questions.

Another aspect not described by the Standard Model is the so-called dark matter. Astronomical observations suggest that only about 15% of the observed matter in the universe is described by the Standard Model in its present form. The rest, called dark due to not being visible to us, could be explained by different extensions of the Standard Model. A prominent example of such BSM extensions are supersymmetric theories, postulating an additional particle for every particle in the Standard Model, the super-partners. Many other theories have been proposed, but so far, experiments have not been able to determine which ones might be realized in nature.

In order to identify the shortcomings of the Standard Model, it is important to make precise predictions that experimental data can be compared against.

1.3 Quantum Chromodynamics and Colliders

In the Standard Model, the strong force is described by QCD. The theory introduces three distinct color charges to the quarks and corresponding anticharges to the antiquarks. The name color is chosen in analogy to how three different colors, say red, green and blue, can add up to a colorless white state. The color charges allow the particles to form color-neutral bound states, the so-called hadrons. These can be mesons, formed from a quark–antiquark pair with a color and the corresponding anti-color, or baryons, which are combinations of the three colors, forming a "white" state. More exotic combinations from combining even more quarks are possible.

QCD is a so-called non-abelian gauge theory, which means that the gluons that are mediating the strong force, can interact with each other. This is different from QED, since photons do not carry electric charges and thus don't interact directly. The coupling parameter of the strong force, α_s , depends on the energy scales at which the force is probed. While the electromagnetic coupling becomes larger at larger energies, the strong coupling becomes smaller, leading to asymptotic freedom: at high energies, the dynamics of color-

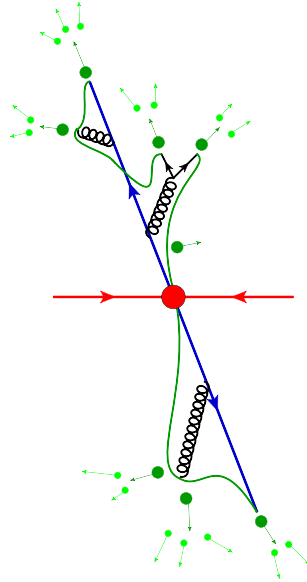


Figure 2: Schematic picture of an electron–positron collision. The red lines depict the incoming electron and positron, which then scatter into a quark–antiquark pair depicted in blue. Additional QCD radiation is emitted in the final state, which then hadronizes to form color-neutral particles shown in green.

charged particles is well described by a perturbative expansion in its coupling parameter, and individual color-charged particles can interact. At low energies, corresponding to large distances, this perturbative expansion breaks down, and colored particles are confined in color-neutral composite objects, i.e., hadrons.

Hadrons are primarily classified by their net quark content, like two up and one down quark for the proton. These so-called valence quarks set some quantum numbers, notably that the hadron charge is the sum of the valence quark charges. In addition there is a sea of shorter-lived particles: gluons needed to bind the quarks, and extra quark–antiquark virtual fluctuations. More and more sea can be observed when the resolution scale is increased. The quark and gluons constituents of a hadron are collectively called partons.

In order to study QCD at particle colliders, different approaches can be taken. We can collide color-neutral objects like electrons and positrons, and look at final states that include colored partons. Such a collision is schematically depicted in Fig. 2. The main component of this collision event is depicted by the red blob, which is the hard process. It can be calculated in perturbation theory and gives a certain probability of the depicted transition of an electron–positron pair to a quark–antiquark as a function of the momenta. Due to the fact that these partons are accelerated charges, there will be additional radiation. Here,

only final state radiation is depicted in the form of gluons being emitted from the outgoing quarks and antiquarks. Due to color confinement, a hadronization needs to take place, converting quarks and gluons into color-neutral hadrons, depicted in green.

Another approach to study QCD and other theories at colliders is the use of hadron colliders like the Large Hadron Collider (LHC) at CERN, which collides protons at very high energies. The interaction of hadrons is then governed by the interactions of their constituents, the quarks and gluons. In contrast to electron–positron collisions, it is thus crucial to model the chances of finding specific partons within the proton. Since there are color charges in the initial state, there are also QCD emissions of the incoming partons. As the colliding particles contain multiple partons, there can also be multiple parton interactions that need to be described.

1.4 Event Generators

In order to predict the outcome of particle collision events, general purpose event generators have been developed. The aim of these programs is to simulate collisions as precisely as possible, while taking all relevant aspects of a collision into account. For hadron–hadron collisions, the relevant physics that need to be modeled can be grouped into the following categories:

Hard scattering At the core of the event, there is typically a hard scattering process, with a high characteristic energy or momentum transfer. This process is modeled in perturbation theory, which is an expansion for small coupling parameters. The precise modeling of the hard process is a crucial ingredient to the full event, often determining its general geometry, but many additional aspects need to be modeled to generate a realistic final state.

Parton Distribution Functions and Initial State Radiation In hadron collisions, the incoming beams consist of composite objects, while the hard process is typically modeled on the level of elementary partons. This necessitates the modeling of the distribution of partons within hadrons, given by Parton Distribution Functions (PDFs). On their way towards the hard collision event, the partons can further radiate other particles, which gives rise to Initial State Radiation (ISR). The radiation off initial state partons and PDFs are closely related.

Final State Radiation The final state partons produced in the hard scattering, as well as partons that might have been emitted from the incoming beams, can further radiate partons. This cascade gives rise to the description of so-called jets, collimated sprays of partons (and later hadrons) that might look different depending on the initiating partons.

Soft scattering and Multi Parton Interactions Not every event consists of a hard scattering. Also softer processes can take place, which can either leave the incoming partons intact (elastic) or break them to transition into something else (inelastic). Also, there might be additional interactions on top of a hard interaction that need to be modeled. These effects are important at hadron colliders, where the incoming objects are composite, so that several constituents may interact more or less independently.

Beam remnants While some partons are kicked out of the incoming hadrons, others continue along the original beam directions. Usually, these remnants are color-connected to the rest of the event.

Hadronization After the evolution of radiative cascades originating from the hard process, and from other event components, the transition to color-neutral hadrons needs to be modeled. Unlike both the hard process and the initial and final state radiation, the strong coupling cannot be treated as small in this context, leading to a non-perturbative treatment of this stage. In the Lund string fragmentation model [8], the fragmentation is modeled based on color fields being stretched between the partons. While very few parameters are needed to describe the perturbative evolution, the non-perturbative hadronization is based on models that depend on a larger number of parameters. These need to be chosen to best reproduce the effects observed at collider experiments.

Decays Some of the now color-neutral hadrons generated in this manner might not be stable, but rather decay on their way towards the detectors. These decays are commonly modeled based on known particle properties and plausible extensions where necessary.

All of the mentioned components of a collision event are probabilistic. In order to answer questions like how many particles of a specific type we expect to see in the final state, or how energetic the hardest jet might be, it is necessary to generate a large number of events, and from this extract the probability distribution that describes the observables of interest. The modeling is thus based on pseudo-random numbers, giving rise to the name Monte Carlo event generators.

All projects collected in this thesis are related to Monte Carlo event generators, specifically in the context of PYTHIA [9]. Paper I concerns the tuning of parameters to best describe experimental data, focusing on the case where many parameters are to be optimized simultaneously. Paper II is concerned with the combination of the hard process with the parton shower, and the corresponding modeling uncertainties. Paper III focuses on some underlying assumptions commonly made in the treatment of color in parton showers, and improvements to the parton-shower simulation taking into account the combination of QCD and QED for specific states. Paper IV concerns the perturbative precision of parton

showers. While these are often based on splitting probabilities modeled to the first order in the strong coupling α_s , this paper concerns improvements of parton showers including higher order splitting functions.

2 Matrix Elements and Cross Sections

In classical scattering experiments, the rate of incoming particles that scatter is proportional to the cross-sectional area of the scattering objects. Such scattering cross sections can be measured at collider experiments. In elementary particle collisions, the simple notion of an area might not hold, but based on the interaction properties of the particles, it is still possible to define, calculate and experimentally access cross sections.

2.1 From Quantum Fields to Cross Sections

In order to predict the probability of observing a specific outcome at a collider experiment with specified initial conditions, we can use the scattering matrix or \mathcal{S} matrix. If a given initial state is characterized by $|i\rangle$, for example two proton beams at the LHC, and the outcome or final state is given by $\langle f|$, for example a given parton configuration, the modulus square of the product $\langle f|\mathcal{S}|i\rangle$ gives the probability of a transition from the specified initial to final states: $|\langle f|\mathcal{S}|i\rangle|^2$.

The scattering matrix encodes information about the time evolution of given states. In free theories, where particles do not interact with each other, $\mathcal{S} = \mathbb{1}$. If a theory allows for interactions, the scattering matrix has a second component, $\mathcal{S} = \mathbb{1} + i\mathcal{T}$, where the matrix \mathcal{T} describes deviations from the free theory. The quantity of interest is now the matrix element \mathcal{M} of the matrix \mathcal{T} describing the transition for given $\langle f|$ and $|i\rangle$:

$$\langle f|\mathcal{T}|i\rangle = (2\pi)^4 \delta^4 \left(\sum p_i^\mu - \sum p_f^\mu \right) \mathcal{M}. \quad (1)$$

In this equation, the delta function of the sums of initial and final state momenta ensures energy and momentum conservation in the process, and \mathcal{M} is short for $\langle f|\mathcal{M}|i\rangle$.

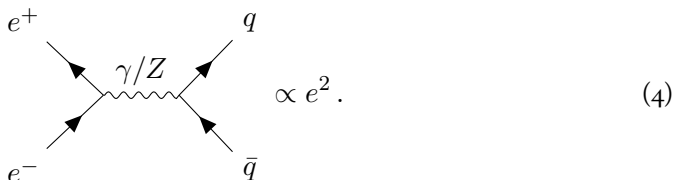
The probability of observing a specified outcome is not given by the matrix element alone. Instead, we need to take into account all possible kinematic configurations that can facilitate the process of interest. This is done by introducing the Lorentz invariant phase space

$$d\Pi \equiv \prod_f \frac{d^3 p_f}{(2\pi)^3} \frac{1}{2E_f} (2\pi)^4 \delta^4 \left(\sum p_i^\mu - \sum p_f^\mu \right), \quad (2)$$

where the product over f labels the final state particles. Together with the flux of incoming particles 1 and 2, this gives the differential cross section

$$d\sigma = \frac{1}{4E_1 E_2 |\vec{v}_1 - \vec{v}_2|} |\mathcal{M}|^2 d\Pi. \quad (3)$$

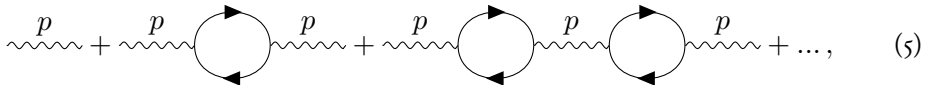
For small coupling parameters, it is then possible to calculate the matrix elements based on perturbation theory. The Feynman rules allow for a pictorial representation of interactions in terms of vertices, external lines and propagators. Each vertex corresponds to one order of the respective coupling constant. For small coupling constants, diagrams with less vertices are dominant. If we look at the scattering of $e^+e^- \rightarrow q\bar{q}$ for example, we find the following leading order diagram:



$$\propto e^2. \quad (4)$$

Due to the fact that this process is mediated by a photon or Z -boson, with two vertices, the matrix element is proportional to e^2 .

One particular higher order contribution is the insertion of fermion loops into the photon propagator, the so-called photon self-energy:



$$+ \dots, \quad (5)$$

which gives contributions of the form

$$1 + \frac{e^2(\mu)}{12\pi^2} \ln \frac{Q^2}{\mu^2} + \left(\frac{e^2(\mu)}{12\pi^2} \ln \frac{Q^2}{\mu^2} \right)^2 + \dots = \frac{e^2(\mu)}{1 - \frac{e^2(\mu)}{12\pi^2} \ln \frac{Q^2}{\mu^2}}. \quad (6)$$

Here, $Q^2 = -p^2$. This resummed correction becomes $e^2(\mu)$ at momenta $Q^2 = \mu^2$. However, for general Q^2 , the coupling is running:

$$e^2(Q^2) \equiv \frac{e^2(\mu)}{1 - \frac{e^2(\mu)}{12\pi^2} \ln \frac{Q^2}{\mu^2}}. \quad (7)$$

This effect comes from the renormalization of a theory, where infinities from high loop momentum integrals are absorbed into the definition of the parameters. The so-called renormalization scale μ , at which the physical value of these parameters is fixed is arbitrary,

and the effective charge should not depend on that choice. This requirement gives rise to the renormalization group equation

$$\mu \frac{de}{d\mu} = \frac{e^3}{12\pi^2} \equiv \beta(e). \quad (8)$$

Equation (7) indicates that for very high energies, corresponding to very low distances, the perturbative description of collisions breaks down.

In QCD, due to the self-coupling of the gluon, the beta function contains both fermion and gluon loops, leading to a qualitatively different behavior. While in QED the coupling increases with energy, the opposite happens in QCD. For the strong coupling $\alpha_s = \frac{g_s^2}{4\pi}$, we have:

$$\alpha_s(Q^2) = \frac{\alpha_s(\mu_R^2)}{1 + \alpha_s(\mu_R^2) \frac{\beta_0}{4\pi} \log \frac{Q^2}{\mu_R^2}} \quad \text{with} \quad \beta_0 = 11 - \frac{2}{3}n_f, \quad (9)$$

where n_f is the number of active flavours. Due to the different sign in this function as compared to the photon case, the strong coupling decreases with increasing scales, leading to asymptotic freedom. In QCD, perturbation theory thus breaks down for low scales, corresponding to large distances, giving rise to confinement of the color charge into hadrons.

In practical calculations, it is not always obvious which value to choose as a reference scale for α_s , giving rise to scale uncertainties. In order to estimate the effect of scale uncertainties, it is customary to vary the scale by a factor of 2 up and down, and take the resulting range as a perturbative uncertainty, which is of higher order in the coupling itself. However, in some situations, for example when the next higher order allows for qualitatively different contributions, the scale band can underestimate the actual uncertainty entailed with the perturbative expansion.

2.2 Hadronic Collisions and Parton Distributions

As discussed above, hadrons are composite objects. Their parton content is given by the valence quarks and antiquarks, and a sea of short-lived gluons and further quark–antiquark pairs. In order to calculate the cross section for hadron collisions, it is useful to relate the hadronic cross section to the partonic cross section of individual partons colliding.

This is the underlying idea of PDFs. They parametrize the probability of finding specific partons in a hadron, carrying a certain fraction of the hadron momentum. Depending on the energy scale at which the hadron is probed, i.e., how hard the collision is, the content of hadrons may look different. In a collision of hadrons A and B , which respectively contain partons a and b with momentum fractions $p_a^\mu = x_a p_A^\mu$, the hadronic cross section $\sigma(AB)$

can be written in terms of different partonic cross sections $\sigma(ab)$ as

$$\sigma(AB) = \sum_{a,b} \int_0^1 \frac{dx_a}{x_a} \int_0^1 \frac{dx_b}{x_b} x_a f_a^A(x_a, \mu) x_b f_b^B(x_b, \mu) \hat{\sigma}(ab), \quad (10)$$

where μ defines a resolution scale, often called factorization scale. Above this scale, partonic interactions are assumed to be described by the partonic cross section $\hat{\sigma}$. Below the scale, the partonic evolution is parametrized by the PDFs, as described below.

At low scales, hadrons mainly consist of their valence quarks, which are carrying a large portion of the hadron momentum. At higher scales, the structure begins to change, and more and more gluons are encountered. With them, also virtual quark–antiquark pairs may be present. Adding up the number of quarks of a given flavour and subtracting the number of corresponding antiquarks should always give the number of valence quarks in the hadron. For protons, which have two up and one down valence quark, this gives

$$\int_0^1 dx (f_d^P(x, \mu) - \bar{f}_d^P(x, \mu)) = 1, \quad \int_0^1 dx (f_u^P(x, \mu) - \bar{f}_u^P(x, \mu)) = 2. \quad (11)$$

Furthermore, the total momentum of a hadron is given by the sum of momenta of all partons

$$\sum_a \int_0^1 dx (x f_a^A(x, \mu)) = 1. \quad (12)$$

Once the parton content of a hadron is parametrized at some (low) resolution scale, the evolution towards higher scales can be calculated perturbatively. The coupled set of differential equations describing this evolution is known as the DGLAP equations [10–12]:

$$\mu \frac{d}{d\mu} \begin{pmatrix} f_i(x, \mu) \\ f_g(x, \mu) \end{pmatrix} = \sum_j \frac{\alpha_s}{\pi} \int_x^1 \frac{d\xi}{\xi} \begin{pmatrix} P_{q_i \leftarrow q_j} \left(\frac{x}{\xi} \right) & P_{q_i \leftarrow g} \left(\frac{x}{\xi} \right) \\ P_{g \leftarrow q_j} \left(\frac{x}{\xi} \right) & P_{g \leftarrow g} \left(\frac{x}{\xi} \right) \end{pmatrix} \begin{pmatrix} f_j(\xi, \mu) \\ f_g(\xi, \mu) \end{pmatrix}, \quad (13)$$

with the splitting functions

$$\begin{aligned}
P_{q \leftarrow q}(z) &= C_F \left[\frac{1+z^2}{[1-z]_+} + \frac{3}{2} \delta(1-z) \right] = \text{---} \rightarrow \begin{array}{l} \nearrow z \\ \searrow 1-z \\ \text{wavy} \end{array} + \dots, \\
P_{q \leftarrow g}(z) &= T_F [z^2 + (1-z^2)] = \text{wavy} \begin{array}{l} \nearrow z \\ \searrow 1-z \end{array}, \\
P_{g \leftarrow q}(z) &= C_F \left[\frac{1+(1-z)^2}{z} \right] = \text{---} \rightarrow \begin{array}{l} \text{wavy} \nearrow z \\ \searrow 1-z \end{array}, \\
P_{g \leftarrow g}(z) &= 2C_A \left[\frac{z}{[1-z]_+} + \frac{1-z}{z} + z(1-z) \right] + \frac{\beta_0}{2} \delta(1-z) \\
&= \text{wavy} \begin{array}{l} \text{wavy} \nearrow z \\ \searrow 1-z \end{array} + \dots
\end{aligned} \tag{14}$$

Here, β_0 is the same as above. The QCD color factors $C_F = 4/3$, $T_F = 1/2$ and $C_A = 3$ are discussed in more detail below. The plus distribution is defined as

$$\int_0^1 dz \frac{f(z)}{[1-z]_+} \equiv \int_0^1 dz \frac{f(z) - f(1)}{1-z}, \tag{15}$$

while $\frac{1}{[1-z]_+} = \frac{1}{1-z}$ for $z \neq 1$. The plus prescription is necessary to subtract the infrared divergence occurring for soft gluon emissions. Physically, arbitrarily soft gluons are not observable. In a fixed order calculation, the divergence is cancelled by the corresponding gluon loop diagram.

The DGLAP equations and corresponding splitting functions are based on the collinear approximation, i.e., emissions at a small angle, which is very reasonable when it comes to identifying partons within a hadron. However, in general, it is desirable to also describe soft wide-angle emission. Those need some special treatment as discussed in Section 3.2.

3 Parton Showers

Just like matrix elements, parton-shower calculations are crucial ingredients for precise predictions of MCEGs. Both are based on the expansion in small coupling parameters, but come with complementary strengths and weaknesses. Matrix element calculations are complete to a given order in the coupling constant, making them a precise baseline for the hard

process calculation. However, some observables are sensitive to the effect of more than a few vertices, requiring an approximate treatment of arbitrarily many emissions. The parton shower is based on such an approximation, being most suited for describing arbitrarily many soft and collinear emissions. However, well separated, hard emissions are not necessarily well described by parton-shower algorithms.

3.1 Parton Shower Resummation

The structure of collinear QCD emissions from partons, governed by the splitting functions in Eq. (14), is universal. This allows for the concept of parton showers: once a certain cross section is calculated, the universal structure of collinear emissions can be used to dress the state with further emissions from both initial and final state partons. For a process $X \rightarrow Y$ where the final state Y contains quarks, the cross section for the emission of an additional gluon collinear to a quark leg is given by

$$d\sigma(X \rightarrow Y + g) = d\sigma(X \rightarrow Y) \sum_{\text{partons}} C_F \frac{\alpha_s}{2\pi} \frac{dp_{\perp}^2}{p_{\perp}^2} dz \frac{1 + (1-z)^2}{z}. \quad (16)$$

The evolution variable, which was called μ in the DGLAP equations above, is here chosen to be p_{\perp}^2 . In principle, this could be different variables, as long as they become singular when the emitted gluon is collinear to the emitting parton. Other possible choices are the emission angle θ or the virtuality $t = (p_q + p_g)^2$. This choice leads to subleading differences, but the dominant contributions of the shower remain the same.

The emission kernels do in general also depend on the azimuthal angle ϕ of the emission. Here, we use the kernels averaged over this angle, and omit the corresponding $d\phi$.

The factor in Eq. (16) can be interpreted as the probability of emitting a gluon (or another parton with the appropriate splitting function) at a specific scale p_{\perp}^2 ,

$$\mathcal{P}(p_{\perp}^2) = \frac{1}{p_{\perp}^2} \frac{\alpha_s}{2\pi} \int_{z_{\min}}^{z_{\max}} dz P_{i \leftarrow j}(z). \quad (17)$$

It is important to keep in mind that the coupling itself does also depend on the scale, and diverges for low transverse momenta where perturbation theory is no longer a useful approximation. This means that we would run into infinitely many emissions at very low scales. Thus, it is crucial to introduce a lower cut-off in p_{\perp}^2 , below which partons combine to form color-neutral hadronic states, and parton-shower emissions are no longer meaningful. Such a cut-off in p_{\perp}^2 also introduces a lower and upper cut on the energy fraction z . For now, we will not explicitly consider the running of α_s , but in detailed calculations it is included.

Taking a closer look at Eq. (17), we see that the emission probability not only diverges for low transverse momenta. In the case of gluon emissions, it further diverges for soft gluons, due to the $1/z$ term in the denominator of the splitting functions. Integrating over z and p_{\perp}^2 will give rise to logarithmic enhancements of the type $\alpha_s \ln^2 \frac{p_{\perp,\max}^2}{p_{\perp,\min}^2}$. These so-called infrared divergences cancel between the real-emission and loop diagrams, and since arbitrarily soft or collinear radiation is not observable in experiments, their occurrence is not a problem in general. It is just important to define observable quantities in an infrared safe way, i.e., observables should not be sensitive to arbitrarily soft or collinear emissions. As an example, it is reasonable to ask for the probability of emitting a jet with a transverse momentum above a given p_{\perp}^2 scale. On the other hand, asking for the total number of gluons emitted in a process, is ill-defined, if we don't specify a minimal energy or transverse momentum for the gluons.

So far, we have only looked at emission probabilities. However, an emission off a given state can only occur if the state did not already change due to an emission at higher scales. The probability of observing the first emission at a certain value of p_{\perp}^2 should thus be given by the emission rate at that scale times the probability of not having an emission before. This no-emission probability between the starting scale $p_{\perp,\max}^2$ and a scale p_{\perp}^2 is also called Sudakov factor $\Delta(p_{\perp,\max}^2, p_{\perp}^2)$. In order to find its form, we can look at small shifts in the evolution. For such small shifts, the no-emission probability will be given by the no-emission probability up to the shift times one minus the probability of an emission at that scale:

$$\begin{aligned} \Delta(p_{\perp,\max}^2, p_{\perp}^2 + \delta p_{\perp}^2) &= \Delta(p_{\perp,\max}^2, p_{\perp}^2) \left(1 - \int_{p_{\perp}^2}^{p_{\perp}^2 + \delta p_{\perp}^2} \mathcal{P}(p_{\perp}^2) dp_{\perp}^2 \right) \\ &= \Delta(p_{\perp,\max}^2, p_{\perp}^2) - \mathcal{P}(p_{\perp}^2) \delta p_{\perp}^2 \Delta(p_{\perp,\max}^2, p_{\perp}^2). \end{aligned} \quad (18)$$

Comparing this to a Taylor expansion

$$\Delta(p_{\perp,\max}^2, p_{\perp}^2 + \delta p_{\perp}^2) = \Delta(p_{\perp,\max}^2, p_{\perp}^2) + \delta p_{\perp}^2 \frac{d}{dp_{\perp}^2} \Delta(p_{\perp,\max}^2, p_{\perp}^2) \quad (19)$$

allows to identify the derivative of the no-emission probability with respect to the evolution variable p_{\perp}^2

$$\frac{d}{dp_{\perp}^2} \Delta(p_{\perp,\max}^2, p_{\perp}^2) = -\mathcal{P}(p_{\perp}^2) \Delta(p_{\perp,\max}^2, p_{\perp}^2). \quad (20)$$

The solution to this equation is given by

$$\Delta(p_{\perp,\max}^2, p_{\perp}^2) = \exp \left(- \int_{p_{\perp}^2}^{p_{\perp,\max}^2} \mathcal{P}(p_{\perp}^2) dp_{\perp}^2 \right). \quad (21)$$

In spirit, this is very similar to radioactive decays: The decay rate $A = \lambda N$ is proportional to the probability of not having observed a decay earlier, or the number of non-decayed particle if we look at an ensemble of particles, leading to an exponential expression for the left-over fraction of particles $N = N_0 e^{-\lambda t}$ from the initial amount N_0 . In this analogy, the evolution variable p_\perp^2 in a parton shower can be interpreted as a time parameter, where decreasing p_\perp^2 corresponds to increasing time.

Having a closer look at the gluon emission rate, now using the explicit form $z_{\min} = 1 - z_{\max} = \sqrt{p_\perp^2/Q^2}$ for the phase space limits in z and assuming $p_{\perp,\max}^2 = Q^2$, allows us to find

$$\mathcal{P}(p_\perp^2) = \frac{\alpha_s}{2\pi} C_F \frac{1}{p_\perp^2} \int_{\sqrt{p_\perp^2/Q^2}}^{1-\sqrt{p_\perp^2/Q^2}} dz \frac{1+z^2}{1-z} \approx \frac{\alpha_s}{2\pi} C_F \frac{1}{p_\perp^2} \left(\ln \frac{Q^2}{p_\perp^2} + \mathcal{O}(1) \right). \quad (22)$$

Using this in the Sudakov factor gives the dominant contribution

$$\begin{aligned} \Delta(p_{\perp,\max}^2, p_\perp^2) &\approx \exp \left(- \int_{p_\perp^2}^{p_{\perp,\max}^2} \frac{\alpha_s}{2\pi} C_F \frac{1}{p_\perp'^2} \left(\ln \frac{p_{\perp,\max}^2}{p_\perp'^2} \right) dp_\perp'^2 \right) \\ &\approx \exp \left(- \frac{\alpha_s}{4\pi} C_F \ln^2 \frac{p_{\perp,\max}^2}{p_\perp^2} \right), \end{aligned} \quad (23)$$

where the missing contributions are less singular in p_\perp^2 . This is the parton shower equivalent of leading logarithmic resummation.

In order to get a feeling for what this entails physically, we can take a look at the emission rate for the hardest gluon. The requirement that it shall be the hardest means that we need to take the Sudakov factor into account,

$$\Delta(p_{\perp,\max}^2, p_\perp^2) \frac{1}{p_\perp^2} \frac{\alpha_s}{2\pi} P_{g \leftarrow q}(z) \approx \exp \left(- \frac{\alpha_s}{4\pi} C_F \ln^2 \frac{p_{\perp,\max}^2}{p_\perp^2} \right) \frac{1}{p_\perp^2} \frac{\alpha_s}{2\pi} C_F \frac{1+(1-z)^2}{z}. \quad (24)$$

This gives a realistic picture of the scale of the hardest emission, not being too big, as the emission rate is enhanced for small scales, but not being too small either, since the low scale region is suppressed by the Sudakov factor. This interplay between Sudakov factors and emission rates is crucial for describing jets, as the scale of an additional hard jet is governed by the hardest parton emitted from the process.

In contrast to analytic resummation calculations, the parton shower generates splittings explicitly, with full kinematic information, i.e., a certain transverse momentum and energy fraction and also an azimuthal angle. The resulting states generated by the parton shower can thus be used to evaluate any observable that depends on the final state momenta. At

the same time, most parton showers ensure that intermediate states are physical, i.e., that all final particles have the right mass. The splitting of massless partons into a pair of two partons with relative momentum thus requires to adjust also the momentum of (one of) the other momenta in the process, such that energy and momentum conservation is guaranteed at all times. This gives rise to the recoil treatment, as we discuss a bit more later.

By construction, parton showers are unitary, i.e., they do not change the inclusive cross section of the state they act upon. Their effect is rather to distribute the cross section differentially over multiple parton multiplicities. Integrating over the probability of having the hardest emission at some scale above the lower cutoff simply gives one minus the probability of having no emission at all,

$$\begin{aligned} \int_{p_{\perp,\min}^2}^{p_{\perp,\max}^2} dp_{\perp}^2 \mathcal{P}(p_{\perp}^2) \Delta(p_{\perp,\max}^2, p_{\perp}^2) &= \int_{p_{\perp,\min}^2}^{p_{\perp,\max}^2} dp_{\perp}^2 \frac{d}{dp_{\perp}^2} \exp \left(- \int_{p_{\perp}^2}^{p_{\perp,\max}^2} \mathcal{P}(p_{\perp}^2) dp_{\perp}^2 \right) \\ &= 1 - \Delta(p_{\perp,\max}^2, p_{\perp,\min}^2). \end{aligned} \tag{25}$$

This property is interesting when correcting the parton shower with fixed-order matrix elements. Depending on the details of how this is done, the shower unitarity may or may not be preserved.

In practical implementations, parton showers often employ the veto algorithm. A detailed description can be found in e.g. [13]. The basic idea is the following:

- For all partons participating in the evolution: propose next emission scale p_{\perp}^2 based on an overestimate of the splitting function.
- Determine a winner parton i and a new parton j .
- Accept the splitting with a rate $P_{i \leftarrow j} / P_{i \leftarrow j}^{\text{over}}$ to compensate for the overestimation.
- Continue sampling from the current p_{\perp}^2 scale until the pre-defined shower cut-off $p_{\perp,\min}^2$ is reached.

As mentioned above, in contrast to analytic resummation techniques, the parton shower constructs explicit kinematic information for every emission step. This is not possible for pure $1 \rightarrow 2$ splittings, so practically, a third parton needs to take some kinematic recoil to make sure that energy and momentum are conserved while all partons have their physical masses. There are different ways to deal with recoil and to assign an appropriate recoiler. In QCD dipole showers, every parton is connected to one (in the case of quarks) or two (in the case of gluons) color partners. In a dipole picture, these can be used as recoilers.

For initial state radiation, the situation is a bit more complex, since one of the involved partons is actually part of the incoming hadron beam. As discussed above, this mandates

to take PDFs into account. The crucial idea to still study the process of interest is to start at the hard process, and sample emissions towards lower scales. This is known as backwards evolution [14]

$$\mathcal{P}(p_{\perp}^2) = \frac{1}{p_{\perp}^2} \frac{\alpha_s}{2\pi} \int_x^{z_{\max}} dz P_{i \leftarrow j} \frac{\frac{x}{z} f_j(\frac{x}{z}, p_{\perp}^2)}{x f_i(x, p_{\perp}^2)}. \quad (26)$$

3.2 Coherence in Parton Showers

Up to this point, the discussion of parton showers was based on collinear radiation. But as we already saw, the emission of gluons is also softly enhanced, i.e., even wide-angle emissions can have a significant rate if the energy of the emitted gluon is small. The collinear approximation includes this soft radiation as a special case in the collinear limit, but it is not necessarily suitable for describing wide-angle emissions.

For the coherent treatment of soft emissions, it is useful to consider the soft limit. As an example, let us consider a process $X \rightarrow \mu^+ \mu^- \gamma$, i.e. a muon anti-muon pair with four-momenta p^μ and p'^μ is emitting a photon with small momentum k^μ and polarization ϵ_μ^* . The corresponding emission term factorizes as

$$\mathcal{M}_{X \rightarrow \mu^+ \mu^- \gamma} = e \mathcal{W}(p, p'; k, \epsilon) \mathcal{M}_{X \rightarrow \mu^+ \mu^-}, \quad (27)$$

with the so-called eikonal term

$$\mathcal{W}(p, p'; k, \epsilon) = \epsilon_\mu^*(k) \left[\frac{p^\mu}{p \cdot k} - \frac{p'^\mu}{p' \cdot k} \right]. \quad (28)$$

This term is divergent both for small photon momenta k^μ and if the photon becomes collinear to one of the muons. The contribution to the squared matrix element then becomes

$$\begin{aligned} \left[\frac{p^\mu}{p \cdot k} - \frac{p'^\mu}{p' \cdot k} \right]^2 &= -2 \frac{p \cdot p'}{(p \cdot k)(p' \cdot k)} \\ &= -2 \left[\frac{p \cdot p'}{(p \cdot k)(p \cdot k + p' \cdot k)} + \frac{p \cdot p'}{(p' \cdot k)(p \cdot k + p' \cdot k)} \right]. \end{aligned} \quad (29)$$

On the right side of the first line, we see that this still shows the same divergences, but now in just one term, mixing soft and both collinear singularities. In the second line of Eq. (29), the two collinear divergences are separated by partial fractioning, identifying one of the collinear divergences in each term. Both terms are divergent for soft photon emissions, and their sum recovers the correct soft radiation pattern overall.

This partial fractioning of coherent dipole radiation is a convenient baseline for building dipole showers, where the term dipole indicates that the radiation is of $2 \rightarrow 3$ type. Each

of the terms should in the collinear limit recover a collinear splitting kernel, while the sum of both should match the eikonal radiation pattern, avoiding double-counting of soft contributions in the collinear sectors. An additional ingredient to the dipole shower approach is a suitable phase space factorization. The same ingredients are also the baseline for fixed-order subtractions of infrared divergences [15, 16], which allow to calculate next-to-leading order cross sections by making the cancellation of infrared divergences explicit between virtual and real contributions. Thus, subtraction schemes and the corresponding momentum maps can be used for the construction of dipole showers [17–20].

Expressed in angles between the particles, the radiation pattern in Eq. (29) can also be written as

$$W_{pp'} = \frac{1 - \cos \theta_{pp'}}{(1 - \cos \theta_{pk})(1 - \cos \theta_{p'k})}. \quad (30)$$

Analogous to the arguments above, this can be separated into two contributions $W_{pp'} = W_{pp'}^{(p)} + W_{pp'}^{(p')}$ with

$$W_{pp'}^{(p)} = \frac{1}{2} \left(W_{pp'} + \frac{1}{1 - \cos \theta_{pk}} - \frac{1}{1 - \cos \theta_{p'k}} \right), \quad (31)$$

such that $W_{pp'}^{(p)}$ is only divergent if the emitted photon is collinear to p . This can now be integrated over the azimuthal angle, giving

$$\int \frac{d\phi_{pk}}{2\pi} W_{pp'}^{(p)} = \begin{cases} \frac{1}{1 - \cos \theta_{pk}} & \text{if } \theta_{pk} < \theta_{pp'}, \\ 0 & \text{otherwise.} \end{cases} \quad (32)$$

Up to a color factor, this result also holds for gluon emissions, and is the baseline for angular ordering in QCD parton showers [21, 22].

3.3 Dealing with Colour

The QCD splitting functions Eq. (14) contain the factors C_F , C_A and T_F , which originate from the $SU(3)$ color group. Vertices of gluon emissions from a quark line include color factors T_{ij}^a , where i and j label the color of the quark lines, while a labels the color of the gluon. For $SU(3)$ there are $N^2 - 1 = 8$ such generators, commonly written in the standard basis $T^a = \frac{1}{2}\lambda^a$, where λ^a are the Gell-Mann matrices.

Their product when squaring this emission matrix element gives the Casimir operator of the fundamental representation, $\sum_a (T^a T^a)_{ij} = C_F \delta_{ij}$. We have $C_F = \frac{N^2 - 1}{2N}$, so $C_F = \frac{4}{3}$ for $SU(3)$. For gluon emissions from gluons, we get the Casimir in the adjoint representation instead, stemming from the structure constants in the vertex $f^{acd} f^{bcd} = C_A \delta^{ab}$. We

have $C_A = N$, so $C_A = 3$ for $SU(3)$. For a gluon split into a quark–antiquark pair, we find $\text{tr}(T^a T^b) = T_{ji}^a T_{ij}^a = T_F \delta^{ab}$ with the group index $T_F = \frac{1}{2}$.

In parton showers, the large N limit is often used to simplify the color treatment. Every new emission is associated with a new color, such that the dipoles that connect colored partons are unique. A quark is color-connected either to a gluon or to an antiquark, which play the role of spectators in a dipole-shower picture. A gluon carries a fundamental and an anti-fundamental index, so it is connected to two other partons instead. In a dipole shower picture, its radiation is therefore distributed on two dipoles. In the large N limit, the Casimir operators become $C_F = N/2 = C_A/2$, such that quarks radiate half as much as gluons, since they only carry one color instead of two. Taking a look at the Fierz identity

$$\sum_a T_{ij}^a T_{kl}^a = \frac{1}{2} \left(\delta_{il} \delta_{kj} - \frac{1}{N} \delta_{ij} \delta_{kl} \right), \quad (33)$$

we see that corrections to this approximation are suppressed by factors $1/N$, which is why the large N limit is also called leading color limit. In practice, it is beneficial to keep the $N = 3$ value for C_F and use the leading color picture to assign dipole partners. The limit is taken such that $\alpha_s N = \text{const.}$, so C_A can keep its value.

In order to include sub-leading color effects in the parton shower, it is necessary to take sub-leading color connections into account. For the example of a $q\bar{q}g$ state, a leading color shower would have a qg and a $g\bar{q}$ dipole. A full color treatment would require an additional color dipole spanned between q and \bar{q} , contributing sub-leading radiation to the $q\bar{q}gg$ state with a negative sign. The treatment of subleading color effects in dipole showers is an ingredient to Paper III, where it is combined with matrix element corrections as discussed below.

3.4 Parton Showers beyond Leading Order

So far, we have discussed parton evolution at leading order in the strong coupling α_s , characterized by the fact that the splitting functions introduced in Eq. (14) do not depend on the strong coupling. The DGLAP equations can be generalized to higher orders in α_s , giving an expansion

$$P_{i\leftarrow j}(z, \alpha_s) = P_{i\leftarrow j}^{(0)}(z) + \frac{\alpha_s}{2\pi} P_{i\leftarrow j}^{(1)}(z) + \dots, \quad (34)$$

where the $P_{i\leftarrow j}^{(0)}$ correspond to the leading order splitting functions introduced above.

The corresponding corrections to the splitting functions to the first order in α_s have been calculated in [23, 24]. On top of the splitting functions discussed so far, there are also new

contributions for $q \rightarrow q'$ and $q \rightarrow \bar{q}$ splittings that do not exist at leading order, stemming from graphs like


(35)

In the collinear limit, a parton shower implementing next-to-leading order parton evolution should reproduce these equations. The intuitive interpretation of the splitting functions as a branching probability does not extend to higher orders, since the corresponding contributions are not necessarily positive. This means that the parton-shower algorithm needs to be able to also sample negative contributions, which can be achieved employing weighted parton-shower algorithms [25–27]. In these algorithms, events are generated with a corresponding event weight that needs to be taken into account when filling histograms of any observable.

In [28, 29], the inclusion of triple collinear and double soft $1 \rightarrow 3$ splittings has been investigating, taking steps towards a fully differential NLO parton evolution. Such an evolution includes correlated emissions of parton pairs in addition to the usual iterated emission of two partons, and allows to cover more phase space beyond the strict ordering of a leading-order shower. Furthermore, it allows for the reduction of scale uncertainties in shower evolution. The consistent combination of the soft and collinear NLO shower evolution is the topic of Paper IV.

4 Matching and Merging

The terms matching and merging refer to techniques of combining matrix element calculations with parton showers. As we discussed above, the fixed-order matrix element calculation is an expansion in small coupling parameters, and can describe high energy collisions with a few well-separated partons very well. The parton shower is a calculation in all orders in the coupling, so it takes leading logarithmic enhancements into account at any order in the coupling. This is crucial to describe soft and collinear configurations, where the all-order Sudakov factor plays an important role, but it comes with the drawback of being based on the soft and collinear limits, which makes parton showers inaccurate for well-separated jet configurations.

In a combination of matrix elements and parton showers, we would like to combine the advantages of both approaches. Well-separated parton configurations should be described accurately by the full matrix element calculation at fixed order, while parton-shower resummation is kept to treat soft and collinear configurations appropriately.

One of the most straightforward approaches to achieve this matching is the use of matrix

element corrections [30]. The basic idea is to generate an emission using the parton-shower approximation, but to then correct to the actual matrix element emission rate, which is given by the ratio of the squared matrix elements of the underlying state and the state with one additional emission:

$$\frac{\alpha_s}{2\pi} \frac{1}{p_{\perp}^2} P_{g\leftarrow q} \rightarrow \frac{\alpha_s}{2\pi} \frac{1}{p_{\perp}^2} P_{g\leftarrow q} \mathcal{R}^{\text{ME}} \quad \text{with} \quad \mathcal{R}^{\text{ME}} = \frac{|\mathcal{M}_{X+g}|^2}{|\mathcal{M}_X|^2 \sum_q \frac{\alpha_s}{2\pi} \frac{1}{p_{\perp}^2} P_{g\leftarrow q}}. \quad (36)$$

In contrast to the parton-shower approximation, the matrix elements are process dependent, so this method requires a process-specific implementation. If the matrix element ratio for the process of interest happens to be smaller than the parton-shower approximation, the correction can be implemented by a hit & miss approach, so instead of accepting proposed parton-shower emissions with the rate given by the parton-shower kernel, they can be accepted with the rate given by the matrix elements. A complication of this method is that there might be kinematic regions that the parton shower does not fill. These would then also be missing the matrix element correction, since only states that the shower can generate can be corrected. In order to reproduce the full matrix element rate, it is therefore necessary to include such regions. Compared to some other methods, as we will see below, another advantage of matrix element corrections is the fact that not only the emission rate, but also the no-emission rate is corrected. The parton shower therefore keeps its unitary property, such that both the emission rates and the Sudakov factors are corrected.

The method of matrix element corrections can be generalized to different processes and emission types, and also be applied iteratively to higher multiplicity configurations as long as the required matrix element calculations are available [31]. The concept of iterated matrix element corrections is relevant for Paper III in this thesis, where it is applied to fixed-color parton-shower evolution.

A related concept is matrix element matching to parton showers including also virtual corrections, with the most common implementations being MC@NLO [32–34] and POWHEG [35–38]. MC@NLO assumes that the poles in the matrix elements are reproduced by the shower. The shower is subtracted from the real-emission matrix element, and added to the virtual contribution. Once the shower is applied to events generated in this way, the physical distributions are recovered. A drawback of this approach is that some events come with negative weights, making the method less efficient. In POWHEG, real and virtual contributions are combined in one sample, and a first emission is generated with the real-emission matrix element as the splitting function, similar to the matrix-element corrections described above. These NLO matching techniques are very appealing, but do not easily allow for the inclusion of multiple hard emission matrix elements simultaneously, which in turn is the strength of multi-jet merging schemes.

4.1 Multi-jet Merging

An alternative approach to combining matrix element calculations of different final state multiplicities is to generate states according to the different matrix elements, and then to consistently combine and shower them afterwards. In a most naïve approach, one might attempt to combine the different samples by just adding the parton-shower effects to each. However, there are some complications to be kept in mind:

- The parton shower on lower multiplicity samples will generate emissions that are already included in higher multiplicity samples. Just adding these up would lead to an overcounting of emission rates, which should be cured.
- Higher multiplicity matrix element configurations are based on fixed-order calculations, so no logarithmic enhancements are included beyond the fixed order in the coupling. In a consistent combination that retains the advantages of matrix elements and parton showers, we would want to also include the shower resummation effects.
- The coupling parameter in the shower is treated as a scale-dependent quantity. In QCD emissions, low transverse momentum emissions are thus further enhanced. This is not the case in matrix element calculations, requiring further corrections.
- Soft and collinear configurations in the matrix element calculation with multiple partons exhibits infrared divergences. In order to be able to sample phase space points that are distributed according to the matrix elements, these configurations require some mitigation.

The general multi-jet merging strategy for combining matrix element calculations of different multiplicities takes these points into account. When generating the events distributed according to the matrix elements for different parton multiplicities, it is first necessary to define some phase space region in which the fixed-order calculation should be considered, and a complementary region that is exclusively sampled by the parton shower. This introduction of a merging scale cut ensures that divergent contributions from soft and collinear configurations are excluded from the fixed-order calculation, allowing for the phase-space sampling of events without divergent contributions. Thinking in terms of a transverse momentum cut, the scale must be chosen high enough to make sure that the matrix element calculation is efficient, and low enough to make sure that the parton-shower approximation is appropriate in the shower exclusive phase space region, since the soft and collinear limits are more appropriate for lower scales. All emissions up to the multiplicity of the available matrix elements in the hard region should then be described by the matrix elements alone. The shower emissions should only fill emission beyond the matrix element multiplicity, and the region below the merging scale, where no hard matrix element configurations are sampled.

So far, the distributions are then fixed-order correct according to the matrix elements. In order to also retain the resummation effects of the parton shower, all-order effects that the shower would have generated need to be added without changing the fixed-order contributions. Following the question *how would a parton shower have generated this state?* then allows to construct the necessary corrections.

- The Sudakov factors can be taken into account by considering no-emission probabilities. This is possible by assigning weights to the matrix elements with additional emissions, which encode the probability of having parton-shower emissions on the corresponding underlying states before the given configuration could be reached. In order to calculate these, it is necessary to find the lower multiplicity configurations from which a parton shower could have generated the state of interest. Then, these factors can either be calculated analytically [39], or by running the parton shower explicitly and checking whether there would have been an emission or not [40].
- With the shower histories at hand, it is also possible to evaluate the coupling parameters at the scales the shower would have chosen, by applying ratios of the desired coupling parameter divided by the one used in the matrix element calculation. Similarly, for initial state radiation, ratios of PDFs need to be taken into account.
- Finally, the parton shower can be used to generate emissions below the merging scale, and for multiplicities higher than what is available from matrix elements, also for the hard region.

Following this prescription, well-separated jets will be described by the appropriate matrix element rates, while resummation of softer and more collinear configurations will be taken into account by the parton shower. The result might exhibit a dependence on the chosen merging scale though. If it is too high, part of the shower-filled region might not be accurate. If it is too low, the efficient matrix element calculation becomes challenging. Since the matrix element calculations includes all logarithmic terms at a given order in the coupling, and the shower only the leading terms, the correction might also introduce subleading logarithmic terms. If only the emission rates, but not the no-emission probabilities are corrected, this leads to a mismatch, changing the total cross section. Both the parton shower accuracy and the fixed-order accuracy are preserved though, but the mismatch might be visible in differential distributions.

The concept of parton-shower histories is important for the procedure outlined above. Every event sampled from a matrix element calculation comes with a set of momenta, but does not provide a notion of how the particles are connected. In contrast, a parton shower has a notion of which parton was emitted by which, and which spectator took the role of a recoiler in an emission. In order to assign the appropriate merging weights, one can build all possible parton-shower histories, and then use all, or a probabilistically chosen

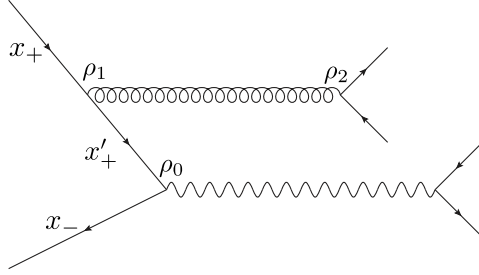


Figure 3: Example of a parton-shower history for a given state with an incoming $q\bar{q}$ pair and $qq\bar{q}\bar{q}$ in the final state. The ρ characterize the scales of the splittings, e.g. a transverse momentum for p_{\perp}^2 ordered showers. The x and x' give the momentum fractions at which the initial state partons are extracted from the incoming beam. The ρ_1 and ρ_2 give the parton-shower scales associated with the parton-shower emissions.

one, to allow for the shower aware merging. To illustrate this, we take a look at an example parton-shower history for the process $q\bar{q} \rightarrow qq\bar{q}\bar{q}$, which is shown in Fig. 3. The variables ρ_1 and ρ_2 correspond to the scales of the splittings, e.g., a transverse momentum for p_{\perp}^2 ordered showers. The values of x and x' give the momentum fractions at which the initial state partons are extracted from the incoming beam.

The differential cross section as given by the matrix element is

$$\frac{d\sigma_{+2}^{\text{ME}}}{d\Phi_{+2}} = x_+ f_+(x_+, \mu_F) x_- f_-(x_-, \mu_F) |\mathcal{M}_{+2}|^2. \quad (37)$$

The corresponding differential parton-shower cross section, generated from a matrix element state $q\bar{q} \rightarrow q\bar{q}$ would instead be given by

$$\begin{aligned} \frac{d\sigma_{+2}^{\text{excl}}}{d\Phi_{+0}d\Phi_1d\Phi_2} &= x'_+ f_+(x'_+, \rho_0) x_- f_-(x_-, \rho_0) |\mathcal{M}_{+0}|^2 \Delta_0(\rho_0, \rho_1) \\ &\quad \frac{\alpha_s(\rho_1)}{2\pi} \frac{x_+ f_+(x_+, \rho_1)}{x'_+ f_+(x'_+, \rho_1)} \frac{x_- f_-(x_-, \rho_1)}{x_- f_-(x_-, \rho_1)} \frac{P_1}{\rho_1} \Delta_1(\rho_1, \rho_2) \\ &\quad \frac{\alpha_s(\rho_2)}{2\pi} \frac{P_2}{\rho_2} \Delta_2(\rho_2, \rho_{\text{ms}}), \end{aligned} \quad (38)$$

where ρ_{ms} is the merging scale. The no-emission probabilities $\Delta(\rho_i, \rho_{i+1})$ occurring in this rate correspond to all partons in the process. For final state partons, these correspond to the Sudakov factor defined in Eq. (21). For initial state partons, the additional PDF ratios in the emission rates need to be taken into account as well.

With these rates, we can now define a weighting factor w that needs to be applied to the higher multiplicity inclusive matrix element to introduce the shower resummation effects:

$$\frac{d\sigma_{+2}^{\text{excl}}}{d\Phi_{+0}d\Phi_1d\Phi_2} = w \frac{d\sigma_{+2}^{\text{ME}}}{d\Phi_{+2}}. \quad (39)$$

By comparing Eq. (37) and Eq. (38) for this particular history and assuming that the coupling factors and PDFs in the matrix element sample are evaluated at the scales μ_R and μ_F respectively, we find

$$\begin{aligned} w &= w_{\alpha_s} w_{\text{pdf}} w_{\text{no-em}} \quad \text{with} \\ w_{\alpha_s} &= \frac{\alpha_s(\rho_1)}{\alpha_s(\mu_R)} \frac{\alpha_s(\rho_2)}{\alpha_s(\mu_R)}, \\ w_{\text{pdf}} &= \frac{f_+(x'_+, \rho_0)}{f_+(x'_+, \rho_1)} \frac{f_+(x_+, \rho_1)}{f_+(x_+, \mu_F)} \frac{f_-(x_-, \rho_0)}{f_-(x_-, \rho_1)} \frac{f_-(x_-, \rho_1)}{f_-(x_-, \mu_F)}, \\ w_{\text{no-em}} &= \Delta_0(\rho_0, \rho_1) \Delta_1(\rho_1, \rho_2) \Delta_2(\rho_2, \rho_{\text{ms}}). \end{aligned} \quad (40)$$

All of these weight factors are expandable as $1 + \mathcal{O}(\alpha_s) + \dots$, such that applying them does not spoil the fixed-order accuracy of the matrix element calculation. At the same time, they introduce the all-order terms that the parton-shower resummation introduces, combining the advantages of both approaches.

4.2 Merging and Unitarity

As discussed above, parton showers are unitary: they distribute the cross section over different parton multiplicities by implementing emission and corresponding no-emission probabilities. In this way, the fixed-order inclusive cross section is not altered by showering. The shower effect on differential distributions that are sensitive to parton emissions can be quite significant though. Calling the total rate inclusive, in the sense that we do not distinguish whether there are further emissions, and the differential rates exclusive, in the sense that we look at a state with a given number of partons without further resolved emissions, the effect of the parton shower is to project inclusive rates onto exclusive distributions.

The multi-jet merging approach as discussed above corrects the emission rates, that a parton shower only approximates. To a given order in the coupling constant, the distributions agree with the fixed-order matrix elements. On the contrary, no-emission probabilities are included using the shower approximations. In unitary multi-jet merging approaches, the merging prescription is adjusted to preserve the unitary property of the shower. The total cross section is not changed when higher multiplicity states are corrected, and the dependence on the merging scale is reduced. This is achieved by not just correcting emission rates, but also no-emission probabilities [41].

Instead of generating no-emission probabilities based on the parton-shower approximation, we can expand the no-emission term:

$$\Delta_0(\rho_0, \rho_{\text{ms}}) = 1 - \int_{\rho_{\text{ms}}}^{\rho_0} d\rho_1 dz \frac{\alpha_s}{2\pi} \frac{P_0^{\text{ME}}}{\rho_1} \Delta_0(\rho_0, \rho_1), \quad (41)$$

where we write the emission probability in terms of the accurate fixed-order rate $P_0^{\text{ME}} = |\mathcal{M}_1|^2/|\mathcal{M}_0|^2$. Focusing on no-emission probabilities for now, and neglecting running coupling and parton flux effects, this relation can be used to write the exclusive cross section as

$$\frac{d\sigma_0^{\text{ex}}}{d\Phi_0} = |\mathcal{M}_0|^2 \Delta_0(\rho_0, \rho_{\text{ms}}) \longrightarrow |\mathcal{M}_0|^2 - \int_{\rho_{\text{ms}}}^{\rho_0} d\Phi_1 |\mathcal{M}_1|^2 \Delta_0(\rho_0, \rho_1). \quad (42)$$

The corresponding one or more parton cross section is

$$\frac{d\sigma_{\geq 1}}{d\Phi_0} = d\Phi_1 |\mathcal{M}_1|^2 \Delta_0(\rho_0, \rho_1), \quad (43)$$

such that the integral over the combined contributions Eqs. (42) and (43) recovers the inclusive lowest multiplicity cross section. If another parton is to be included, we can repeat the same procedure. The exclusive one-parton cross section can be written as

$$\begin{aligned} \frac{d\sigma_1^{\text{ex}}}{d\Phi_0} &= d\Phi_1 |\mathcal{M}_1|^2 \Delta_0(\rho_0, \rho_1) \Delta_1(\rho_1, \rho_{\text{ms}}) \\ &\longrightarrow d\Phi_1 |\mathcal{M}_1|^2 \Delta_0(\rho_0, \rho_1) - d\Phi_1 \Delta_0(\rho_0, \rho_1) \int_{\rho_{\text{ms}}}^{\rho_1} d\Phi_2 |\mathcal{M}_2|^2 \Delta_1(\rho_1, \rho_2), \end{aligned} \quad (44)$$

while the cross section with two or more additional partons is given by

$$\frac{d\sigma_{\geq 2}}{d\Phi_0} = d\Phi_1 \Delta_0(\rho_0, \rho_1) d\Phi_2 |\mathcal{M}_2|^2 \Delta_1(\rho_1, \rho_2), \quad (45)$$

such that upon integration, we still recover the lowest multiplicity cross section as desired. This recipe can be followed for further emissions, as long as the necessary matrix element calculations are available.

So far, the discussion concerned tree level matrix elements, such that emission as well as no-emission rates are described according to their respective lowest fixed-order matrix elements. For these, a merging prescription should avoid overcounting of emission from matrix elements and the parton shower. For a genuine higher order calculation, both tree-level and loop diagrams are included in the matrix element calculations. These introduce desired α_s terms that are only approximated by the shower. Therefore, the corresponding $\mathcal{O}(\alpha_s)$ terms need to be subtracted from the merging weights to avoid spoiling the fixed order accuracy of included matrix element samples. This corresponds to avoiding an overcounting of virtual contributions. The inclusion of NLO matrix elements in different unitary NLO merging prescriptions with their respective uncertainties is the topic of Paper II.

5 Monte Carlo Event Generator Tuning

As discussed in Section 1.4, general purpose event generators aim to provide fully differential predictions of collision events, describing numerous observables simultaneously. The theory and models going into the simulation depend on a number of parameters that need to be adjusted to suitably describe the expected observational data. In adjusting these parameters, it is important to maintain the generality of the simulation. A tune should not be aiming at just describing a certain observable really well while neglecting other effects, but rather provide a set of parameters that is suitable to describe all components of the event reasonably well.

Due to the high number of parameters, and the abundance of experimental data to describe, the task of tuning can be challenging. It is therefore helpful to identify which parameters can be tuned independently of others, and what processes and observables are suitable to be used for the optimization. As an example, electron-positron collisions provide a good baseline for tuning final state radiation and hadronization in the absence of initial state radiation, beam remnants and underlying event effects. In the perturbative parts of the event generation, there are only very few parameters, most notably the coupling constant. By focusing on sufficiently inclusive observables and employing appropriate perturbative input, the coupling can be determined rather independently of other parameters. Hadronization on the other hand is based on models that entail multiple parameters, some of which are more universal than others. Also, the lower cut-off of the parton shower can influence the transition from the perturbative to the non-perturbative regime. It is therefore not always possible to tune one parameter at a time, based on a small set of observables.

A manual tuning approach can be very time-consuming, and requires expert knowledge on both the parameters that are to be tuned, and the experimental data to be employed. Automated tuning approaches have been proposed, one heavily used example being the PROFESSOR package [42] based on the RIVET analysis toolkit [43]. It allows for the efficient optimization of several parameters simultaneously, using an interpolation of the event generator response. The exact definition of the goodness-of-fit function, and the selection and relative weight of the data histograms and bins used as a target distribution for the tune are user-defined.

In Paper I, we address the problem of high dimensional parameter determination, employing an algorithmic splitting of the parameters into subspaces and an automated setting of the weights used in the goodness-of-fit function, enabling a more automated retuning whenever changes in the event generators require it. This makes tunes more reproducible and reduces the influence of user made choices, the impact of which is difficult to access.

6 Outlook

The theme of this thesis are the uncertainties of event generators, and the included publications take steps in different directions. Based on these, further studies are possible, and a few ideas are given below.

The first paper presents an algorithm for the tuning of event generators for high dimensional parameter spaces. The method allows for tuning with reduced human interaction, and therefore also for tuning different models with a similar bias. Applying this procedure to different models could be used to identify mismodeling, since the origin of differences is less likely to be attributed to better or worse tuning. In the automated assignment of weights, the difference between pure parton shower and matched/merged predictions could be used to reduce the weight of observables that are very sensitive to these kinds of corrections. Furthermore, the over-representation of correlated data could be addressed in future work.

The second paper concerns scale and scheme variations in unitarized NLO merging. In addition to the commonly employed renormalization scale variations, a scheme variation can be used by reweighting to estimate algorithmic uncertainties. Further sources of uncertainties could be included in a similar fashion, but would require some redesign of the parton-shower algorithm, for example variations of the merging scale, the factorization scale in conjunction with the shower starting scale or the shower cut-off. This improved uncertainty budget could also be used as a baseline for an NLO tune, ideally leading to a more universal result due to less perturbative bias on non-perturbative models.

In the third paper, we present a shower framework allowing for fixed-color parton evolution with QCD/QED interference effects through matrix element corrections. We find these effects to be small in a simple test case, but see that electroweak effects can be very significant. Further phenomenological studies could help to refine this outcome, by looking at more general configurations and including also initial state radiation. The developments in this project could also facilitate parton-shower matching to fixed color hard-scattering events, since these are used as a starting point for the fixed-color shower evolution. Another interesting application of the presented framework is the use for fixed color shower deconstruction.

In the fourth paper, we address the question of how to combine triple-collinear and double-soft corrections to parton showers. The net effect of including these corrections is small when employing a reasonable leading order shower, and helps to reduce the uncertainties. The implementation of a complete NLO parton evolution seems possible based on this approach. Besides being valuable as such, this would also facilitate the use of modified subtraction schemes at $\mathcal{O}(\alpha_s^2)$.

7 Overview of Publications

Here, I briefly summarize each paper in the thesis and specify my individual contributions.

Paper I: High dimensional parameter tuning for event generators

Johannes Bellm, Leif Gellersen

Eur.Phys.J.C 80 (2020) 1, 54. E-print: arXiv:1908.10811 [hep-ph]

LU-TP-19-40, MCNET-19-20

We present an algorithm that allows to tune Monte Carlo Event Generators for high dimensional parameter spaces by splitting the parameter space algorithmically and performing PROFESSOR tunes on the resulting subspaces. We test the algorithm in ideal conditions and in real life examples.

Johannes Bellm proposed the project and the basic algorithm, which we then developed together. The implementation was a joint effort. I performed the test under ideal conditions, where we tune to a data set that what previously generated with a known set of parameters, that we aimed to recover. I also performed the PYTHIA 8 LEP tune. In the manuscript, I wrote section 2, contributed to section 3, and wrote the relevant parts of sections 4 and 5.

Paper II: Scale and scheme variations in unitarized NLO merging

Leif Gellersen, Stefan Prestel

Phys.Rev.D 101 (2020) 11, 114007. E-print: arXiv:2001.10746 [hep-ph]

LU-TP-20-03, MCNET-20-04

In this paper, we discuss possible pit-falls in defining the perturbative uncertainty of unitarized next-to-leading order multi-jet merging predictions. For this purpose, we define and implement different unitarized NLO merging schemes and discuss consistent variations of renormalization scales. We find that both the central prediction and the scale uncertainties are affected, but largely overlap. Differences can be comparable to scale uncertainties though, even for well-separated jets.

Based on the UNLOPS implementation in PYTHIA 8, I implemented the alternative NLO matching schemes and consistent renormalization scale variations in different parts of the calculation, and produced the results and plots for the paper. Of the manuscript, I wrote the *Theory and Implementation* and *Application and Results* sections.

Paper III: Coloring mixed QCD/QED evolution

Leif Gellersen, Stefan Prestel, Michael Spannowsky

To be submitted to SciPost Phys. E-print: arXiv:2109.09706 [hep-ph]

IPPP/21/30, LU-TP-21-41, MCNET-21-16

In this paper, we investigate the effect of QCD/QED interference in parton showers. For this purpose, we develop a shower including QED, QCD at fixed color, and tree-level matrix element corrections for fixed color configurations. We find QCD/QED interference effects to be small in a simple test case.

My contributions to this project are the implementation of a fixed color shower mode for the DIRE parton shower in PYTHIA 8, and the kinematic matrix element corrections based on fixed color states. I furthermore adapted the necessary matrix element plugin for the simple test case. I generated the results and figures, wrote large parts of section 2, and wrote section 3 of the paper.

Paper IV: Disentangling soft and collinear effects in QCD parton evolution

Leif Gellersen, Stefan Höche, Stefan Prestel

To be submitted to Phys.Rev.D. E-print: arXiv:2110.05964 [hep-ph]

FERMILAB-PUB-21-483-T, LU-TP-21-44, MCNET-21-17

We introduce a method for the consistent removal of overlapping singularities in QCD parton evolution at the next-to-leading order in the strong coupling. Using an implementation in the DIRE parton shower, we analyze the numerical impact of the genuine tripe-collinear corrections for quark pair emission in $e^+e^- \rightarrow \text{hadrons}$.

For this project, I implemented the consistently assembled next-to-leading order quark to quark splittings based on the previous NLO shower machinery in the DIRE shower for PYTHIA 8, and generated the corresponding results. The paper was written in collaboration.

Further contributions

In addition to the four papers listed above, I made additional contributions that are not included in this thesis. These include technical developments in PYTHIA, especially around the handling of event weights and merging, and contributions to the upcoming PYTHIA 8.3 manual. The developments of Papers II, III and IV are and will be made available in PYTHIA.

I also contributed to the following report.

Self-consistency of backwards evolved initial-state parton showers

Leif Gellersen, Davide Napoletano, Stefan Prestel

Les Houches 2019: Physics at TeV Colliders: Standard Model Working Group Report

E-print: arXiv:2003.01700 [hep-ph]

8 Acknowledgements

First of all, I would like to thank the whole Theoretical High Energy Physics group in Lund for the kind and open atmosphere I enjoyed over the last four years. Due to the Covid-19 pandemic and the restrictions that came with it, I have seen all of you much less than I would have liked during the last months. Special thanks go to my fellow PhD students! I wish you all the best with your theses and for your future.

Next, I would like to thank my supervisor Stefan. Thank you for your guidance, encouragement and expertise, and for finding time for our projects even when you were busy with other duties. Thanks also to Malin and Leif for your support and advice, especially during my first time in Lund.

Many thanks also to my other collaborators Johannes, Michael and Stefan. I enjoyed working with you, and learned a lot from our projects.

Thanks also to MCnet and its members for the meetings and schools, where I learned a lot and met many great people. Thanks as well to the Pythia collaboration, for welcoming me and for being a great team.

I would also like to thank my fellow students at NDR, it was great to work with you. I would especially like to mention Brian, Andrew, Camille, Lea, Smita and Mattias.

Also, thanks to Torbjörn, Stefan and Frauke for the time you spent on proofreading the introduction and providing feedback.

Finally, thanks to my family and friends for your support. Thanks a lot to Baptiste, Elena and Smita for the fun we had together. And warmest thanks to Wiebke and Linnéa for your support especially during the last months of writing this thesis.

References

- [1] M. E. Peskin and D. V. Schroeder, *An introduction to quantum field theory*. Westview, Boulder, CO, 1995.
- [2] M. D. Schwartz, *Quantum Field Theory and the Standard Model*. Cambridge University Press, 3, 2014.
- [3] J. Campbell, J. Huston, and F. Krauss, *The Black Book of Quantum Chromodynamics: A Primer for the LHC Era*. Oxford University Press, 12, 2017.
- [4] A. Buckley *et al.*, “General-purpose event generators for LHC physics,” *Phys. Rept.* **504** (2011) 145–233, arXiv:1101.2599 [hep-ph].
- [5] A. Einstein, “Ist die Trägheit eines Körpers von seinem Energieinhalt abhängig?,” *Annalen der Physik* **323** no. 13, (1905) 639–641. <https://onlinelibrary.wiley.com/doi/abs/10.1002/andp.19053231314>.
- [6] ATLAS Collaboration, G. Aad *et al.*, “Observation of a new particle in the search for the Standard Model Higgs boson with the ATLAS detector at the LHC,” *Phys. Lett. B* **716** (2012) 1–29, arXiv:1207.7214 [hep-ex].
- [7] CMS Collaboration, S. Chatrchyan *et al.*, “Observation of a New Boson at a Mass of 125 GeV with the CMS Experiment at the LHC,” *Phys. Lett. B* **716** (2012) 30–61, arXiv:1207.7235 [hep-ex].
- [8] B. Andersson, G. Gustafson, G. Ingelman, and T. Sjöstrand, “Parton fragmentation and string dynamics,” *Physics Reports* **97** no. 2, (1983) 31–145. <https://www.sciencedirect.com/science/article/pii/0370157383900807>.
- [9] T. Sjöstrand, S. Ask, J. R. Christiansen, R. Corke, N. Desai, P. Ilten, S. Mrenna, S. Prestel, C. O. Rasmussen, and P. Z. Skands, “An introduction to PYTHIA 8.2,” *Comput. Phys. Commun.* **191** (2015) 159–177, arXiv:1410.3012 [hep-ph].
- [10] Y. L. Dokshitzer, “Calculation of the Structure Functions for Deep Inelastic Scattering and e^+e^- Annihilation by Perturbation Theory in Quantum Chromodynamics,” *Sov. Phys. JETP* **46** (1977) 641–653.
- [11] V. N. Gribov and L. N. Lipatov, “Deep inelastic $e p$ scattering in perturbation theory,” *Sov. J. Nucl. Phys.* **15** (1972) 438–450.
- [12] G. Altarelli and G. Parisi, “Asymptotic Freedom in Parton Language,” *Nucl. Phys. B* **126** (1977) 298–318.

- [13] T. Sjöstrand, S. Mrenna, and P. Z. Skands, “PYTHIA 6.4 Physics and Manual,” *JHEP* **05** (2006) 026, [arXiv:hep-ph/0603175](#).
- [14] T. Sjöstrand, “A Model for Initial State Parton Showers,” *Phys. Lett. B* **157** (1985) 321–325.
- [15] S. Catani and M. H. Seymour, “A General algorithm for calculating jet cross-sections in NLO QCD,” *Nucl. Phys. B* **485** (1997) 291–419, [arXiv:hep-ph/9605323](#). [Erratum: *Nucl.Phys.B* **510**, 503–504 (1998)].
- [16] S. Catani, S. Dittmaier, M. H. Seymour, and Z. Trocsanyi, “The Dipole formalism for next-to-leading order QCD calculations with massive partons,” *Nucl. Phys. B* **627** (2002) 189–265, [arXiv:hep-ph/0201036](#).
- [17] Z. Nagy and D. E. Soper, “A New parton shower algorithm: Shower evolution, matching at leading and next-to-leading order level,” in *Ringberg Workshop on New Trends in HERA Physics 2005*, pp. 101–123. **1**, 2006. [arXiv:hep-ph/0601021](#).
- [18] M. Dinsdale, M. Ternick, and S. Weinzierl, “Parton showers from the dipole formalism,” *Phys. Rev. D* **76** (2007) 094003, [arXiv:0709.1026](#) [hep-ph].
- [19] S. Schumann and F. Krauss, “A Parton shower algorithm based on Catani-Seymour dipole factorisation,” *JHEP* **03** (2008) 038, [arXiv:0709.1027](#) [hep-ph].
- [20] S. Plätzer and S. Gieseke, “Coherent Parton Showers with Local Recoils,” *JHEP* **01** (2011) 024, [arXiv:0909.5593](#) [hep-ph].
- [21] G. Marchesini and B. R. Webber, “Simulation of QCD Jets Including Soft Gluon Interference,” *Nucl. Phys. B* **238** (1984) 1–29.
- [22] S. Gieseke, P. Stephens, and B. Webber, “New formalism for QCD parton showers,” *JHEP* **12** (2003) 045, [arXiv:hep-ph/0310083](#).
- [23] G. Curci, W. Furmanski, and R. Petronzio, “Evolution of Parton Densities Beyond Leading Order: The Nonsinglet Case,” *Nucl. Phys. B* **175** (1980) 27–92.
- [24] W. Furmanski and R. Petronzio, “Singlet parton densities beyond leading order,” *Physics Letters B* **97** no. 3, (1980) 437–442. <https://www.sciencedirect.com/science/article/pii/037026938090636X>.
- [25] S. Höche, S. Schumann, and F. Siegert, “Hard photon production and matrix-element parton-shower merging,” *Phys. Rev. D* **81** (Feb, 2010) 034026. <https://link.aps.org/doi/10.1103/PhysRevD.81.034026>.
- [26] S. Plätzer and M. Sjödal, “The Sudakov Veto Algorithm Reloaded,” *Eur. Phys. J. Plus* **127** (2012) 26, [arXiv:1108.6180](#) [hep-ph].

- [27] L. Lönnblad, “Fooling Around with the Sudakov Veto Algorithm,” *Eur. Phys. J. C* **73** no. 3, (2013) 2350, arXiv:1211.7204 [hep-ph].
- [28] S. Höche and S. Prestel, “Triple collinear emissions in parton showers,” *Phys. Rev. D* **96** no. 7, (2017) 074017, arXiv:1705.00742 [hep-ph].
- [29] F. Dulat, S. Höche, and S. Prestel, “Leading-Color Fully Differential Two-Loop Soft Corrections to QCD Dipole Showers,” *Phys. Rev. D* **98** no. 7, (2018) 074013, arXiv:1805.03757 [hep-ph].
- [30] M. Bengtsson and T. Sjöstrand, “Coherent Parton Showers Versus Matrix Elements: Implications of PETRA - PEP Data,” *Phys. Lett. B* **185** (1987) 435.
- [31] W. T. Giele, D. A. Kosower, and P. Z. Skands, “A simple shower and matching algorithm,” *Phys. Rev. D* **78** (2008) 014026, arXiv:0707.3652 [hep-ph].
- [32] S. Frixione and B. R. Webber, “Matching NLO QCD computations and parton shower simulations,” *JHEP* **06** (2002) 029, arXiv:hep-ph/0204244.
- [33] S. Hoeche, F. Krauss, M. Schönherr, and F. Siegert, “A critical appraisal of NLO+PS matching methods,” *JHEP* **09** (2012) 049, arXiv:1111.1220 [hep-ph].
- [34] V. Hirschi, R. Frederix, S. Frixione, M. V. Garzelli, F. Maltoni, and R. Pittau, “Automation of one-loop QCD corrections,” *JHEP* **05** (2011) 044, arXiv:1103.0621 [hep-ph].
- [35] P. Nason, “A New method for combining NLO QCD with shower Monte Carlo algorithms,” *JHEP* **11** (2004) 040, arXiv:hep-ph/0409146.
- [36] S. Frixione, P. Nason, and C. Oleari, “Matching NLO QCD computations with Parton Shower simulations: the POWHEG method,” *JHEP* **11** (2007) 070, arXiv:0709.2092 [hep-ph].
- [37] S. Alioli, P. Nason, C. Oleari, and E. Re, “A general framework for implementing NLO calculations in shower Monte Carlo programs: the POWHEG BOX,” *JHEP* **06** (2010) 043, arXiv:1002.2581 [hep-ph].
- [38] S. Plätzer and S. Gieseke, “Dipole Showers and Automated NLO Matching in Herwig++,” *Eur. Phys. J. C* **72** (2012) 2187, arXiv:1109.6256 [hep-ph].
- [39] S. Catani, F. Krauss, R. Kuhn, and B. R. Webber, “QCD matrix elements + parton showers,” *JHEP* **11** (2001) 063, arXiv:hep-ph/0109231.
- [40] L. Lönnblad, “Correcting the color dipole cascade model with fixed order matrix elements,” *JHEP* **05** (2002) 046, arXiv:hep-ph/0112284.

- [41] L. Lönnblad and S. Prestel, “Unitarising Matrix Element + Parton Shower merging,” *JHEP* **02** (2013) 094, arXiv:1211.4827 [hep-ph].
- [42] A. Buckley, H. Hoeth, H. Lacker, H. Schulz, and J. E. von Seggern, “Systematic event generator tuning for the LHC,” *Eur. Phys. J. C* **65** (2010) 331–357, arXiv:0907.2973 [hep-ph].
- [43] A. Buckley, J. Butterworth, D. Grellscheid, H. Hoeth, L. Lönnblad, J. Monk, H. Schulz, and F. Siegert, “Rivet user manual,” *Comput. Phys. Commun.* **184** (2013) 2803–2819, arXiv:1003.0694 [hep-ph].